

Insights into memory effect mechanisms of layered double hydroxides with solid-state NMR spectroscopy

Received: 11 July 2022

Accepted: 7 October 2022

Published online: 14 October 2022

Check for updates

Li Jin¹, Xiaoyuan Zhou¹, Fang Wang¹, Xiang Ning¹, Yujie Wen¹ , Benteng Song¹, Changju Yang¹, Di Wu², Xiaokang Ke¹ & Luming Peng^{1,3,4}

Layered double oxides (LDOs) can restore the parent layered double hydroxides (LDHs) structure under hydrous conditions, and this “memory effect” plays a critical role in the applications of LDHs, yet the detailed mechanism is still under debate. Here, we apply a strategy based on ex situ and in situ solid-state NMR spectroscopy to monitor the Mg/Al-LDO structure changes during recovery at the atomic scale. Despite the common belief that aqueous solution is required, we discover that the structure recovery can occur in a virtually solid-state process. Local structural information obtained with NMR spectroscopy shows that the recovery in aqueous solution follows dissolution-recrystallization mechanism, while the solid-state recovery is retro-topotactic, indicating a true “memory effect”. The amount of water is key in determining the interactions of water with oxides, thus the memory effect mechanism. The results also provide a more environmentally friendly and economically feasible LDHs preparation route.

Layered double hydroxides (LDHs), a class of bimetallic hydroxide materials, have received a lot of research attention because of their applications in many fields, such as adsorbents, catalysts and energy storage materials^{1–5}. One of the most attractive features of LDHs materials is the so-called “memory effect”: layered double oxides (LDOs) formed by calcining LDHs at a moderately high temperature, can restore the original LDHs structure in contact with the aqueous solution containing appropriate anions (Fig. 1)^{6–9}. Memory effect has a variety of applications, including pollutant removal¹⁰, preparations of new LDHs¹¹, activation of catalysts¹², as well as structural investigations of LDHs¹³. It is therefore important to understand the details on the structure change during the LDHs regeneration.

Despite enormous efforts to investigate this issue by applying methods such as X-ray Photoelectron Spectroscopy (XPS), X-ray absorption fine structure spectroscopy (XAFS) and X-ray diffraction (XRD)^{14–17}, detailed information on this process is still missing, and the

memory effect mechanism remains a topic of intense debate in the literature^{18–20}. One of the main reasons behind this controversy is the complicated nature of the structures in the LDHs regeneration process, in which considerable turbostratic disorder and stacking faults in the hydroxide or oxide layers may be present, making structural characterization challenging²¹. Thus, characterization techniques that can provide local environments of LDOs and LDHs are required to fill the missing piece of the puzzle.

Solid state nuclear magnetic resonance (NMR) spectroscopy is a powerful tool with which to provide quantitative, nuclear specific and local structural information of solids at the atomic level^{22–26}. Consequently, it should be an ideal approach to give the short-range order of LDOs and LDHs. In principle, ¹H, ²⁷Al, ¹⁷O, and ²⁵Mg NMR spectroscopy can all be used to explore the structure of Mg and Al-containing LDHs; however, ¹⁷O and ²⁵Mg NMR investigations are very challenging and were rarely applied because of their low natural abundances, relatively

¹Key Laboratory of Mesoscopic Chemistry of MOE, School of Chemistry and Chemical Engineering, Nanjing University, Nanjing 210023, China. ²College of Food Science and Engineering/Collaborative Innovation Center for Modern Grain Circulation and Safety/Key Laboratory of Grains and Oils Quality Control and Processing, Nanjing University of Finance and Economics, Nanjing 210023, China. ³Jiangsu Key Laboratory of Vehicle Emissions Control, Nanjing University, Nanjing 210093, China. ⁴Frontiers Science Center for Critical Earth Material Cycling (FSC-CEMaC), Nanjing University, Nanjing, Jiangsu 210023, China. ✉ e-mail: luming@nju.edu.cn

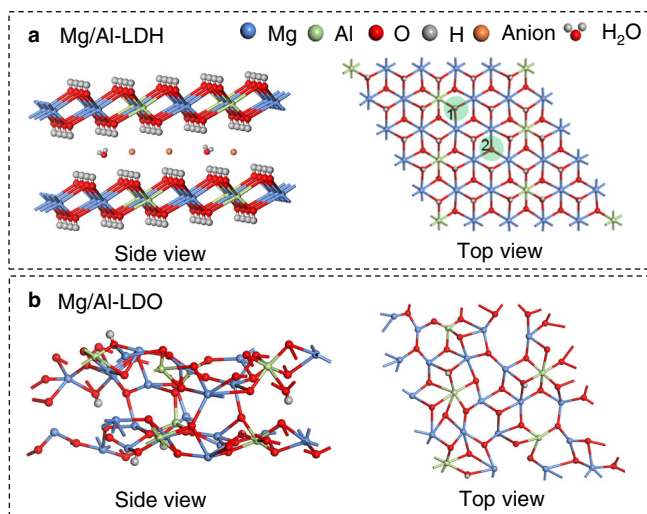


Fig. 1 | Structure of Mg/Al-LDH and Mg/Al-LDO. Schematic structure of Mg/Al-LDH (a) and Mg/Al-LDO (b) in the side and top views. The shaded green circles show the local environment of Mg_2AlOH (1) and Mg_3OH (2).

low gyromagnetic ratios and quadrupolar nature^{13,27}. Therefore, ^1H and ^{27}Al solid-state NMR spectroscopy represent more convenient approaches to illustrate the structure of LDHs. Different H species, including Mg_3OH , Mg_2AlOH , MgAl_2OH , and interlayer water in Mg/Al-LDH can be distinguished by using ^1H NMR spectroscopy^{28–30}, and 4- and 6-coordinated Al ions can be easily differentiated with ^{27}Al NMR spectroscopy. In this work, we combine ex situ and in situ ^1H and ^{27}Al NMR spectroscopy, and demonstrate this approach can track the detailed structure change during the LDHs regeneration, even in real time. A solid-state recovery scheme is found to be possible, which involve different mechanism compared to recovery in aqueous solutions. The results indicate the importance of the amount of water in controlling the interactions and reactions between oxide and water, which are widely occurring in nature and man-made systems.

Results

Mg- and Al-containing LDH (Mg/Al-LDH) with Al molar ratio of 20% was prepared by co-precipitation method (Supplementary Table 1)^{28,31}, and the corresponding Mg/Al-LDO was obtained by heating Mg/Al-LDH at 450 °C. The material before calcination shows a typical XRD pattern of LDH, and the interlayer distance ($d_{003} = 0.80$ nm) suggests that the sample is a typical NO_3^- intercalated LDH (Fig. 2a)³². After calcination, two peaks at 43.2° and 62.6° can be attributed to (200) and (220) reflections of the MgO structure, respectively, while no diffraction peak due to the Al_2O_3 phase can be observed, indicating that Al^{3+} ions are well dispersed in the MgO-like structure and Mg/Al-LDO is formed³³. Fig. 2b–e shows the microstructures and morphologies of the Mg/Al-LDH and Mg/Al-LDO materials. Mg/Al-LDH exhibits a laminar structure, while the well-defined morphology is retained in Mg/Al-LDO.

Due to large ^1H - ^1H dipolar interactions, deuteration of the samples were performed to decrease the proton density and thus ^1H homonuclear dipolar coupling, and to improve spectral resolution at medium to low spinning speed in solid-state NMR experiments²⁸. High-resolution ^1H NMR spectra can be obtained on deuterated Mg/Al-LDH samples (Supplementary Fig. 1), and analysis shows that they provide quantitative information on the relative concentration of Mg_3OH and Mg_2AlOH species (Supplementary Fig. 2). The ^1H magic-angle spinning (MAS) NMR spectrum of Mg/Al-LDO shows a weak peak at approx. -0.1 ppm and a shoulder at -0.9 ppm, both of which can be assigned to residual hydroxyl groups after thermal treatment (Supplementary Fig. 3a)³⁴. The ^{27}Al MAS NMR spectrum of Mg/Al-LDO exhibits two

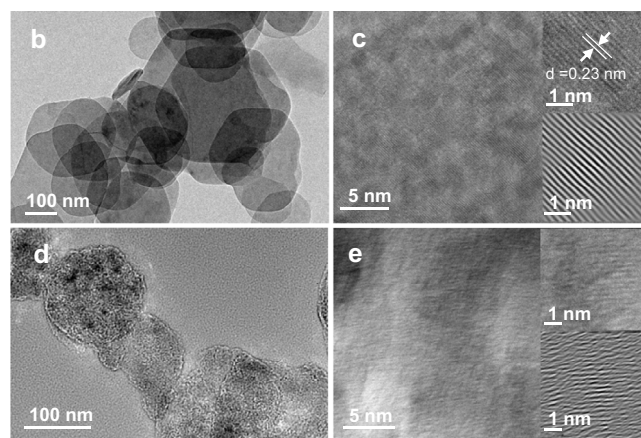
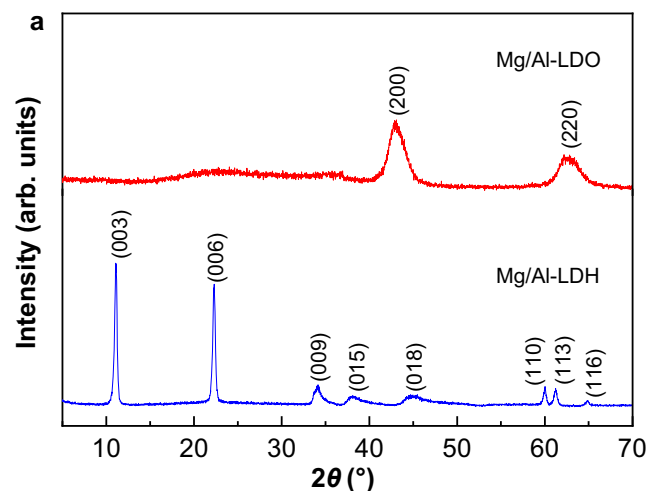


Fig. 2 | XRD patterns and electron microscopy images of Mg/Al-LDH and Mg/Al-LDO. a XRD patterns of Mg/Al-LDH and Mg/Al-LDO. TEM (b) and HRTEM (c) images of Mg/Al-LDH. TEM (d) and HRTEM (e) images of Mg/Al-LDO.

broad resonances with maxima at -74 and 10 ppm, corresponding to 4- and 6-coordinated Al ions, which is consistent with the observation in the literature (Supplementary Fig. 3b)³⁵.

Ex situ XRD studies

After mixing Mg/Al-LDO with NaNO_3 solution in D_2O during a conventional recovery process (mass ratio of Mg/Al-LDO to D_2O is -1:100), the ex situ XRD patterns of the resulting solids after a specific rehydration time t (10 min to 48 h) are shown in Fig. 3, and the cell parameters refined from this data are given in Supplementary Table 2. The (003) reflection of LDH starts to appear after 10 min, and shifts to lower angles with increasing t , suggesting that nitrate anions are gradually intercalated into the interlayer spaces and the distance between lamellae is increased. The intensities of the (003) reflections of the samples with relatively short t (10 min to 6 h) are less intense than those of the Mg/Al-LDH and the reflections ((200) and (220)) due to MgO-like phase (LDO) are still present, suggesting that the recovery process is far from being finished and the regenerated LDH phase is not well crystallized at this stage. The peaks owing to LDO become much weaker after $t = 20$ h and disappear $t = 28$ h, suggesting complete conversion of LDO and the reconstruction of the LDH structure is virtually completed, which can be concluded from the similar characteristic diffraction line with the Mg/Al-LDH. The (003) reflection peaks for the sample with a longer t (28 to 48 h) become narrower with increasing time, indicating further crystallization of the LDH structure. No peak due to any intermediate species is observed, indicating that the transformation from Mg/Al-LDO to Mg/Al-LDH does not involve

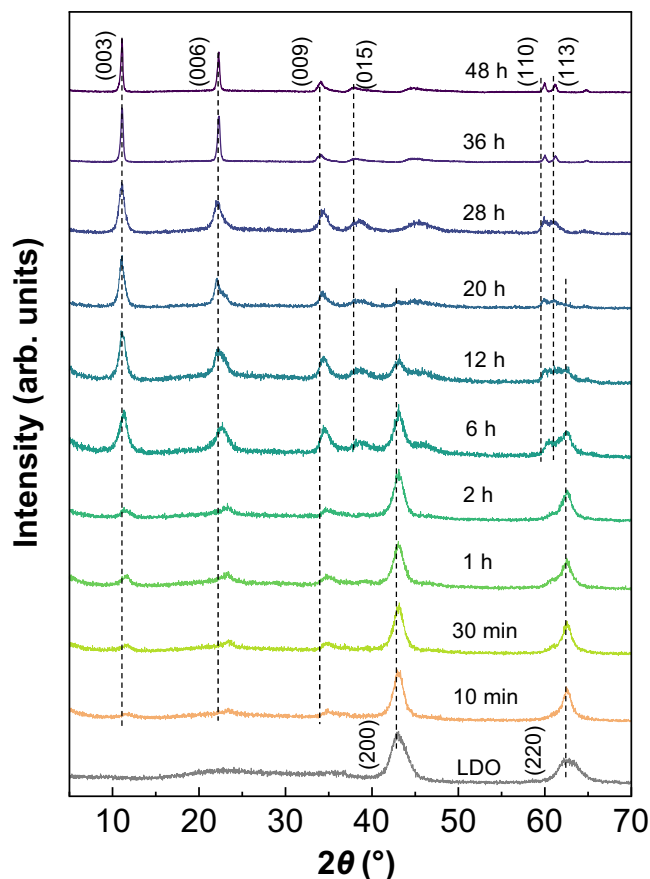


Fig. 3 | Ex-situ XRD patterns of rehydrated Mg/Al-LDO. XRD patterns of the resulting solids after mixing Mg/Al-LDO with NaNO₃ solution in D₂O during a conventional recovery process (mass ratio of Mg/Al-LDO to D₂O is -1:100) for a specific rehydration time *t* (10 min to 48 h).

another crystalline phase, and such recovery may occur in a single step. TG/DTG profiles and nitrate concentrations show the LDH structure is regenerated after 36 h (see Supplementary Fig. 4, Supplementary Table 3 and related discussion in Supplementary Information), and this recovery time is slightly longer than the time suggested by XRD (28 h). Nonetheless, details in the structure change on molecular level are still missing.

Ex situ solid-state NMR studies

Thus, the corresponding ex situ ¹H and ²⁷Al NMR spectra were also obtained (Fig. 4). The NMR data change dramatically with different rehydration time *t*, implying that NMR spectroscopy is a sensitive method to probe the structure evolution for the memory effect. Even with a short *t* of 10 min, the relative intensity of the peak at 74 ppm in the ex situ ²⁷Al NMR spectrum decreases significantly, while the signal at around 10 ppm increases, indicating that a large fraction of 4-coordinated Al ions has been converted to 6-coordinated Al species (Fig. 4b). At the same time, the ex situ ¹H NMR spectral intensity is significantly stronger than Mg/Al-LDO, indicating that rich hydroxyl groups are generated by water dissociation (Fig. 4a). With increasing *t* (10 min to 2 h), a broad ¹H resonance with maximum at 3.6 ppm is observed, along with a sharper peak at 1.3 ppm and a shoulder at an even lower frequency (0.8 ppm), indicating multiple ¹H chemical environments.

The relative intensity of the ex situ ²⁷Al NMR peak at 74 ppm further decreases at *t* = 2–20 h while the ²⁷Al NMR resonance at 10 ppm becomes narrower, implying that the conversion from 4-coordinated Al to 6-coordinated Al continues during this time. The 4-coordinated

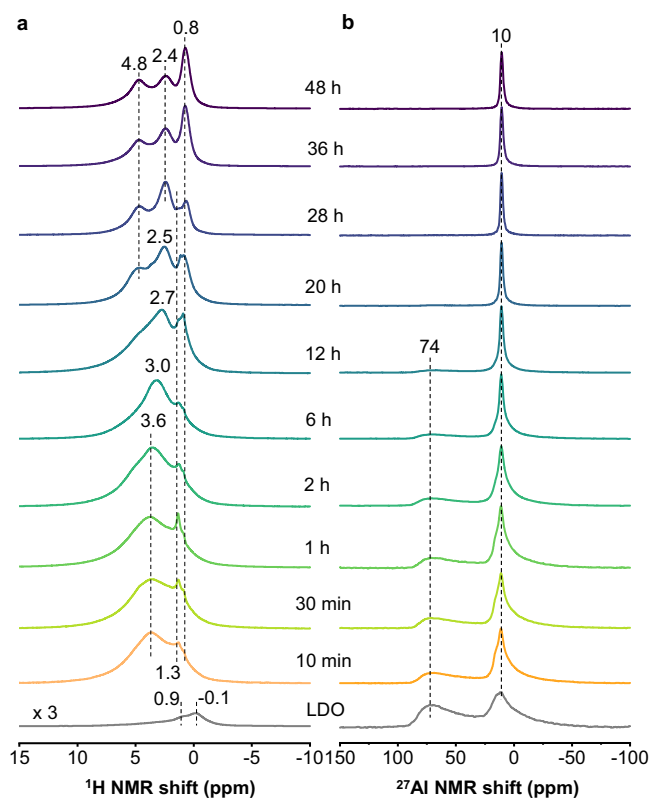


Fig. 4 | Ex situ NMR spectra of rehydrated Mg/Al-LDO. **a** ¹H and **b** ²⁷Al MAS NMR spectra of rehydrated Mg/Al-LDO for different rehydration time *t*. Mg/Al-LDO was rehydrated with NaNO₃ in D₂O solution (mass ratio of LDO to D₂O is 1:100).

Al ions can no longer be observed at 20 h, suggesting that the above conversion process completes. Meanwhile, the ex situ ¹H NMR resonances show a noticeable change: the signal at 3.6 ppm shifts to 3.0 ppm at *t* = 6 h, and further to 2.7 ppm at *t* = 12 h, which can be attributed to the significant short-range structure changes resulting from the formation of Mg₂AlOH species in Mg/Al-LDH structure²⁵. The resonance at -0.8 ppm becomes more prominent after 12 h, which can be ascribed to Mg₃OH species in the Mg/Al-LDH phase. At *t* = 20 h, the ¹H NMR spectrum is much better resolved, and the major resonances are observed at 0.8–1.3, 2.5 and 4.8 ppm, which can be readily assigned to Mg₃OH, Mg₂AlOH and interlayer water in Mg/Al-LDH, respectively²⁵.

At a longer rehydration time *t* (28–48 h), ex situ ²⁷Al NMR spectra show a single sharp peak at 10 ppm and exhibit no obvious change with time, indicating that all the Al ions are 6-coordinated at this stage. However, the ex situ ¹H NMR spectra exhibit significant changes. The relative intensities of the peaks at -0.8 and 2.4 ppm vary at different mixing time. At *t* = 28 h, the peak at 2.4 ppm is the strongest peak, while the resonance at 0.8 ppm becomes the most intense peak in the spectra of the samples with *t* at 36 and 48 h (Supplementary Fig. 5). The increase of the fraction of Mg₃OH sites in this final stage (*t* = 28–48 h) suggests that more Mg₃OH species are generated than Mg₂AlOH, and thus the formation of Mg₃OH is slower than Mg₂AlOH in the recovery process. These NMR data are very different from XRD results, which provide long-range order: the XRD reflections owing to LDO disappear after *t* = 28 h and only peaks due to LDH remain (Fig. 3), suggesting complete conversion of LDO to LDH while the NMR results show that the short-range structure is still changing. Furthermore, no sharp component at 1.3 ppm can be observed after 36 h and only one strong peak at 0.8 ppm is present, implying that the peak at 1.3 ppm should correspond to an intermediate species.

These ¹H NMR spectral assignments are further supported by ¹H-²⁷Al TRansfer of Population in DOuble Resonance (TRAPDOR)

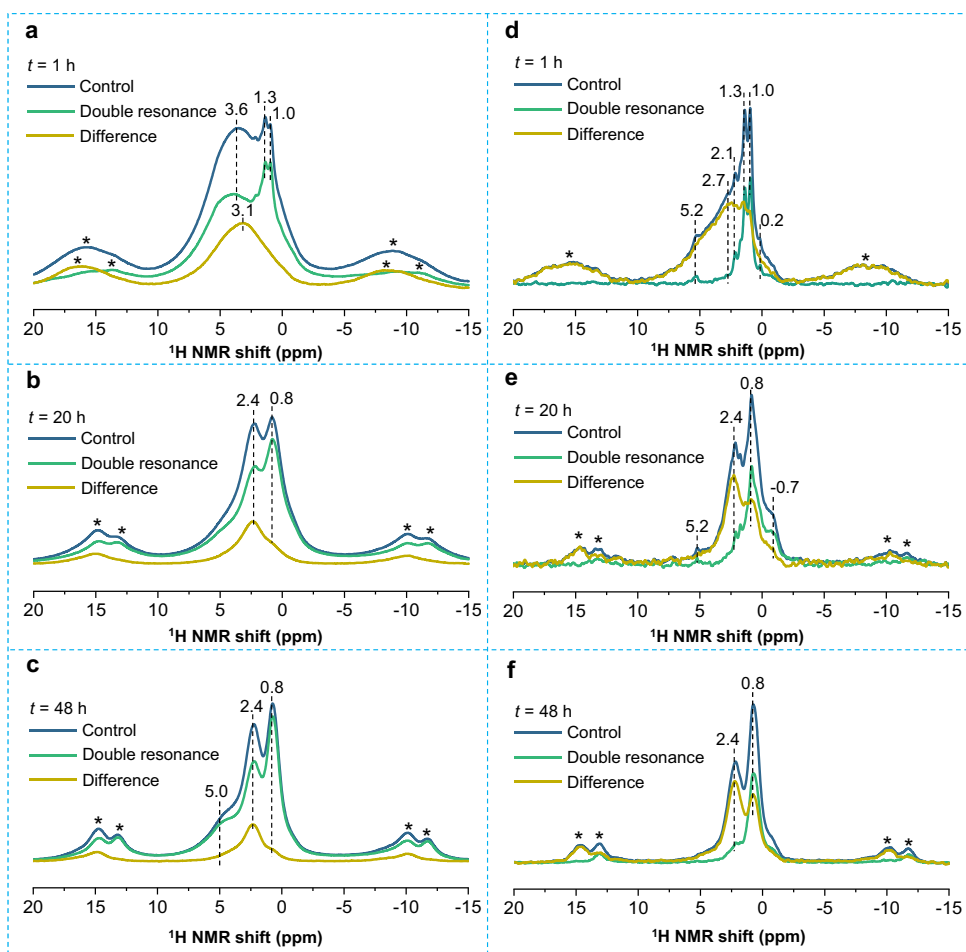


Fig. 5 | ^1H - ^{27}Al TRAPDOR NMR data of rehydrated Mg/Al-LDO. ^1H - ^{27}Al TRAPDOR NMR spectra of Mg/Al-LDO with a rehydration time $t = 1$ (a), 20 (b) and 48 h (c) and a recoupling time of 0.2 ms. ^1H - ^{27}Al TRAPDOR NMR spectra of Mg/Al-LDO with a

rehydration time $t = 1$ (d), 20 (e) and 48 h (f) and a recoupling time of 2 ms. Mass ratio of Mg/Al-LDO to D_2O : -1:100; spinning speed: 5 kHz.

experiments (Fig. 5)³⁶. The TRAPDOR control spectrum of Mg/Al-LDO after conventional recovery ($t = 1$ h), shows a broad peak at -3.6 ppm with relatively sharp components at 1.0 and 1.3 ppm (Fig. 5a). The double resonance spectrum, acquired with continuous irradiation on ^{27}Al of 0.2 ms, exhibits significant intensity decrease for the broad peak at 3.1 ppm, indicating that this peak is due to hydroxyl species close to Al ions. On the other hand, the sharp peaks appear in the double resonance spectrum with similar intensity compared to the control spectrum, indicating that these resonances correspond to local environments not very close to Al atoms. According to the chemical shifts, the resonances at 1.0 and 1.3 ppm can be assigned to hydroxyl sites around only Mg atoms. At $t = 20$ h, the control spectrum shows two major resonances at 0.8 and 2.4 ppm (Fig. 5b). The corresponding double resonance spectrum exhibits significant spectral intensity decrease for both the signals at 0.8 and 2.4 ppm, while the latter has a greater effect. Since the LDH structure has been formed at this stage according to diffraction data, the two signals at 0.8 and 2.4 ppm should be ascribed to Mg_3OH and Mg_2AlOH sites in hydroxide sheets. The former (0.8 ppm) shows a non-zero TRAPDOR effect due to Al in the 4th coordination shell (i.e., H-O-Mg-O-Al), which increases with longer ^{27}Al irradiation time (Fig. 5d–f). Finally, at $t = 48$ h, well-resolved peaks at 2.4 and 0.8 ppm along with a relatively strong shoulder at 5.0 ppm can be observed, corresponding to Mg_2AlOH and Mg_3OH in the hydroxide sheets and interlayer water in the well-crystallized LDH structure, respectively (Fig. 5c). According to the optimized LDH structure, the H-Al distances in H-O-Al (Mg_2AlOH) and H-O-Mg-O-Al (Mg_3OH) environments are predicted to be 2.5 and 4.2/5.2 Å (Supplementary Fig. 6),

which is in agreement with the relatively large and small TRAPDOR fractions for the peaks at 2.4 and 0.8 ppm, respectively.

In situ solid state NMR studies

In order to further explore the details of structural changes associated with the “memory effect”, NaNO_3 solution in D_2O was added to the NMR rotor packed with Mg/Al-LDO and in situ ^1H and ^{27}Al MAS NMR spectra were acquired to investigate the structure change in real time (Fig. 6 and Supplementary Figs. 7, 8). In this case, the mass ratio of LDO to D_2O is -1:1, while this amount of water is enough for the hydroxylation of LDO as well as interlayer water in the LDH structure according to the composition of Mg/Al-LDH (Supplementary Fig. 4 and Supplementary Table 1). Since only a small amount of solution is added, this is a “solid-state recovery” attempt to generate Mg/Al-LDH from Mg/Al-LDO.

In the first 10 min of rehydration, in addition to the major peak at 4.8 ppm due to water, two weak shoulders can be clearly observed at -3.6 and 1.3 ppm, which are assigned to hydroxyl groups close to both Mg and Al ions, respectively, according to the ^1H NMR shift²⁵. Even with a short rehydration time t of just 2 min, these two resonances are already present, implying that water molecules dissociate very rapidly to form hydroxyl species at some highly active sites, possibly Lewis sites ($\text{Mg}^{2+}-\text{O}^{2-}$ and $\text{Al}^{3+}-\text{O}^{2-}$ acid-base pairs) at the edge or surface of Mg/Al-LDO³⁷. Diffusion of water should also occur in this first 2 min time period, which is probably accelerated by rapid magic angle spinning. In this 10 min, 4-coordinated Al shows little change in the ^{27}Al NMR spectra, while 6-coordinated Al signal shows a

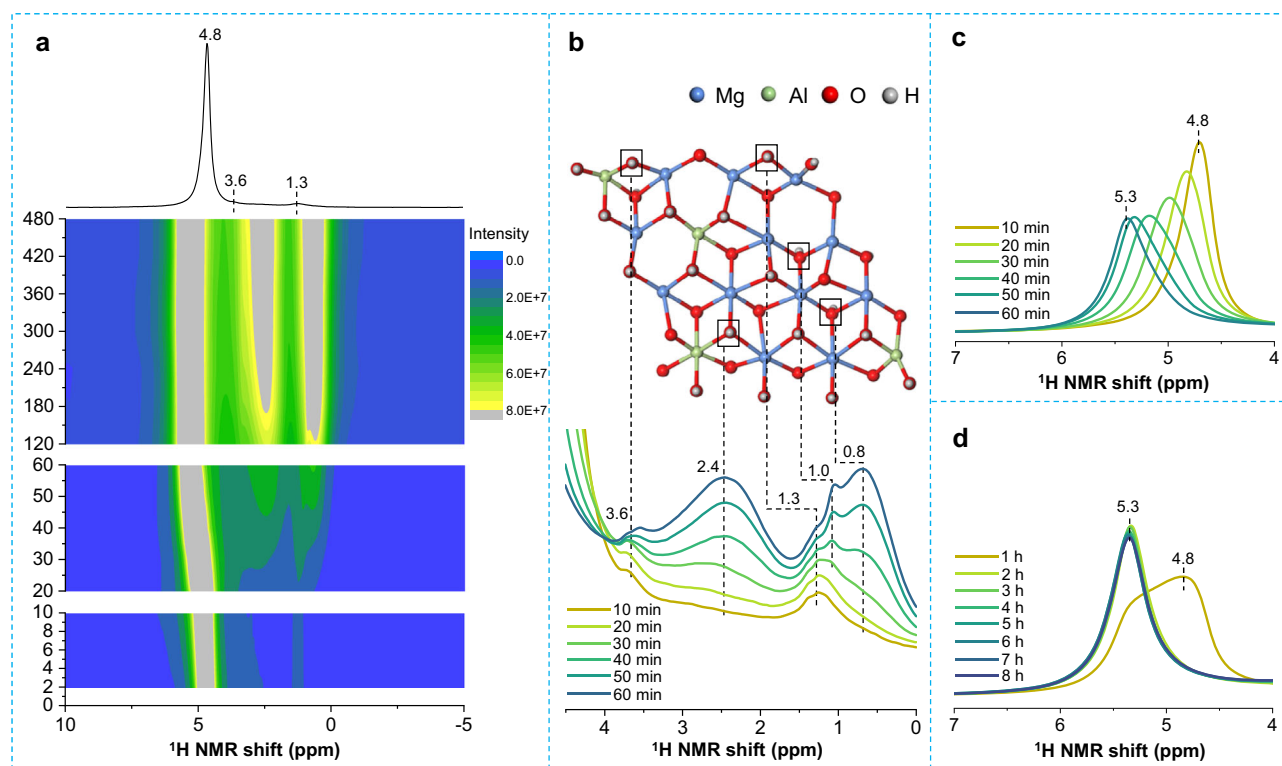


Fig. 6 | In situ ^1H NMR spectra of rehydrated Mg/Al-LDO. **a** 2D in situ ^1H MAS NMR spectra of rehydrated Mg/Al-LDO (mass ratio of LDO to D_2O is 1:1). The 1D spectrum shown on top corresponds to a rehydration time of 2 min. Each spectrum during rehydration time $t = 2$ –10 min, 10–60 min and 2–8 h takes ~ 2 min, 10 min and 1 h to collect, respectively, by adjusting the acquisition

numbers. **b** Overlay of in situ ^1H MAS NMR spectra in (a) in the range of 0–4.5 ppm with $t = 10$ –60 min along with the corresponding spectral assignments. **c** Overlay of in situ ^1H MAS NMR spectra in (a) in the range of 4–7 ppm with $t = 10$ –60 min. **d** Overlay of in situ ^1H MAS NMR spectra in (a) in the range of 4–7 ppm with $t = 1$ –8 h.

slight increase, indicating that some Al species in Mg/Al-LDO, which are not detected due to large quadrupolar interactions, are converted to 6-coordinated Al ions during this time (Supplementary Fig. 8).

With a longer rehydration time t of 10 to 60 min, broader peaks with peak maxima at -2.4 and 0.8 ppm emerge and increase significantly with time, implying that the occurrence of a continuous water dissociation process. These characteristic resonances can be readily assigned to Mg_2AlOH and Mg_3OH species in the hydroxide sheets of the newly formed Mg/Al-LDH structure, respectively²⁵. XRD pattern of the sample right after collecting the in situ ^1H NMR spectrum at $t = 60$ min confirms the presence of LDH phase in addition to the LDO phase at this stage (Supplementary Fig. 9). In contrast, the intensities of the relatively sharp components at 3.6 and 1.3 ppm do not change much during this period of time. The results imply that these species are intermediate and are further converted to Mg_2AlOH and Mg_3OH in the Mg/Al-LDH structure, while new hydroxyl sites on the edge/surface of Mg/Al-LDO are formed at the same time, resulting in nearly unchanged intensity for such signals. Another relative narrow peak at 1.0 ppm, presumably due to Mg_3OH species in a slightly different environment, can also be observed with $t > 40$ min. Furthermore, the peak due to water gradually shifts to a higher frequency of 5.3 ppm with time. Because water molecules in the interlayer regions are known to resonate at 4.8 ppm²⁵, such shift to a higher frequency indicates that more water molecules resonate at a higher frequency, presumably due to hydrogen bonding to the hydroxyl species^{38–40}. For in situ ^{27}Al MAS NMR spectra, the intensity of the peak at 74 ppm decreases, while a significant intensity growth and linewidth narrowing can be observed for the peak at ca. 10 ppm, indicating the formation and further crystallization of the Mg/Al-LDH phase.

When the rehydration time is extended from 60 to 480 min, continuous and simultaneous increase in the intensities of the broad

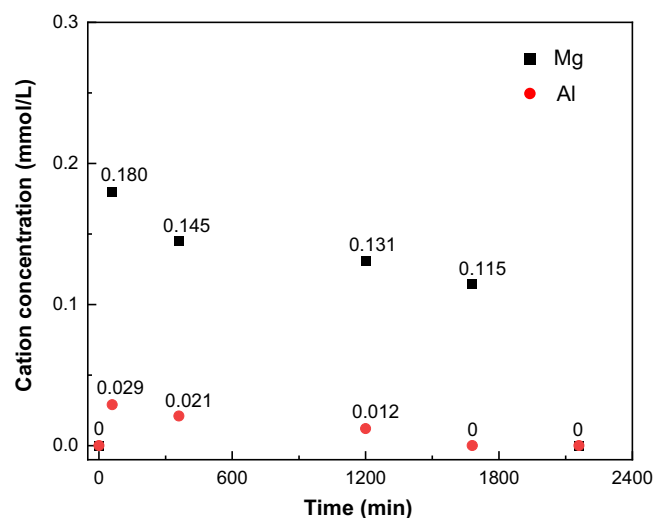


Fig. 7 | The cation concentration changes in the supernatant solution. The cation concentration in the supernatant solution after centrifugation of the sample in a conventional recovery with rehydration time t of 0 min, 60 min, 360 min (6 h), 1200 min (20 h), 1680 min (28 h) and 2160 min (36 h).

peaks centered at -2.4 and 0.8 ppm can be observed before 360 min, indicating the further generation of the Mg_2AlOH and Mg_3OH species in the Mg/Al-LDH structure. However, there is very little change in spectral intensity after 360 min for the peaks arising from Mg_2AlOH and Mg_3OH (Supplementary Figs. 10, 11), indicating that the dissociation of water has completed and the vast majority of the LDO structure is converted to LDH during the first 6 h. After $t = 6$ h, almost no signal

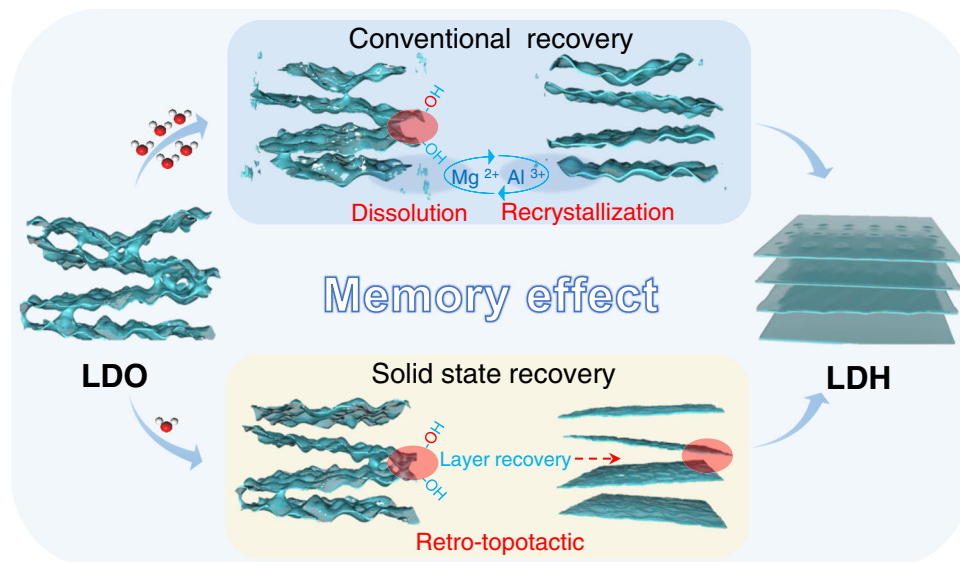


Fig. 8 | Schematic representation of memory effect mechanisms. The above route from LDO to LDH represents conventional recovery with a large amount of water, in which dissolution occurs first, followed by recrystallization of LDH

structure. In the bottom route, LDO structure is regenerated more rapidly in a retro-topotactic process with the presence of a small quantity of water.

arising from 4-coordinated Al ions can be observed in in situ ^{27}Al NMR spectra (Supplementary Fig. 8). The disappearance of the LDO phase is confirmed by the XRD data on the sample right after obtaining its in situ NMR spectrum at $t = 6$ h (Supplementary Fig. 9). To the best of our knowledge, it is the first example that LDO can restore the parent LDH structure with a very small amount of solution in a virtually solid-state process, while a large amount of water was always considered necessary for such structure conversion from LDO to LDH.

The nature of memory effect

By applying solid-state NMR spectroscopy, the details in the structural evolution from LDO to LDH are revealed, even in real time with in situ spectroscopy. Since both the variations of local structure (i.e., Mg_3OH vs Mg_2AlOH) and recovery time in conventional recovery in aqueous solution and solid-state recovery are significantly different, distinct mechanisms should be involved in the two recovery processes. It is worth noting that our solid-state recovery was performed in an NMR rotor spinning at a very high frequency (20 kHz), therefore, LDO rehydration (mass ratio of Mg/Al -LDO to D_2O is -1:1) was also performed at a zero MAS rate (Supplementary Fig. 12). Similar XRD patterns corresponding to LDH structure are observed for the two samples with $t = 6$ h, suggesting that MAS does not account for the faster recovery in the solid-state. Because the relative concentrations of Mg_3OH and Mg_2AlOH significantly change during conventional recovery (Fig. 4), the concentrations of Mg and Al ions in the supernatant solution after centrifugation of the sample were measured. Relatively high concentrations of Mg and Al ions are found in the solution in the early and middle stage of rehydration in conventional recovery, while the concentrations of Al and Mg ions only decrease to 0 in the final stage with $t = 28$ h or longer (Fig. 7 and Supplementary Table 4). Thus, the formation of LDH in conventional recovery should be ascribed to the partial dissolution of LDO (in a large amount of water) followed by recrystallization of LDH from the solution. This two-step process is expected to be more time-consuming than a direct structure conversion in solid-state recovery. It is also clear that Mg ions in the LDO dissolve more easily compared to Al ions, and the ratios of Mg to Al in the solution (>6) is always higher than the original ratio in LDO ($\text{Mg}/\text{Al} = 4$) before the conversion is finished, resulting in partially recovered Al-rich solid material, therefore, a stronger peak at 2.4 ppm

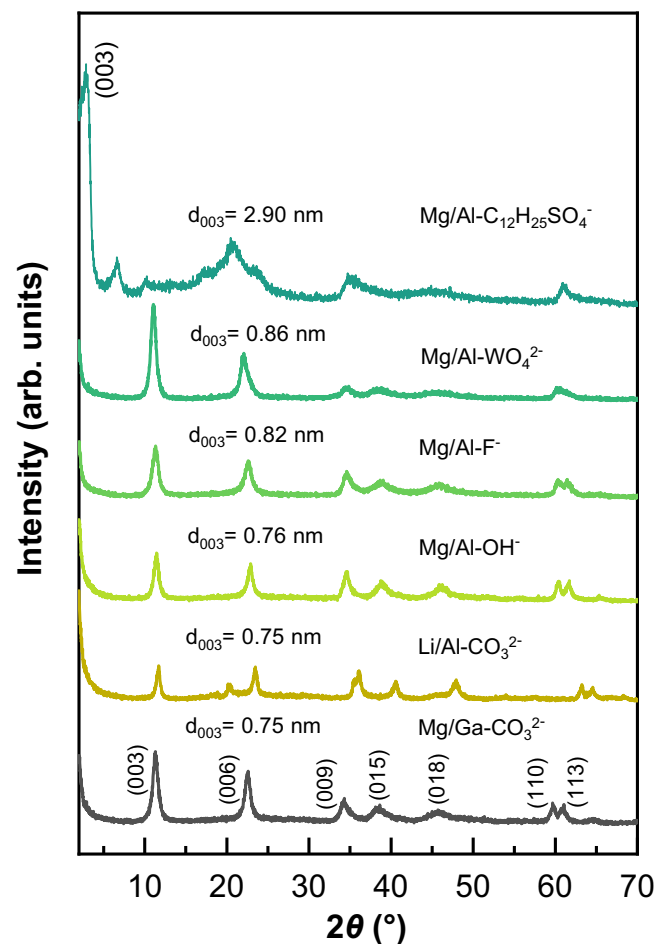


Fig. 9 | XRD patterns of regenerated LDHs. XRD patterns of LDHs with different anions or cations prepared with a solid-state recovery process from corresponding LDOs.

for Mg₂AlOH than the peak at 0.8 ppm for Mg₃OH (e.g., $t = 28$ h, Supplementary Fig. 5).

The detailed mechanisms of the memory effect of LDH at the atomic scale can be summarized in Fig. 8. When the mass ratio of LDO to D₂O is -1:100, the interactions of water with oxides are dominated by the dissolution process and both Mg and Al ions are dissolved, while the Mg²⁺ concentration is higher in solution. Therefore, in the LDH recrystallization process, the formation of Mg₃OH sites is slower than the Mg₂AlOH sites, and the whole structure recovery process takes long time (~36 h, Fig. 4 and Supplementary Fig. 13) to finish with such dissolution-recrystallization mechanism. In a solid-state recovery process with the mass ratio of LDO to D₂O of -1:1, water molecules can rapidly dissociate on the high active sites to form intermediate hydroxyl species. With enough water molecules for the presence in the interlayer region in LDH, the continuous opening of the interlayer space can be realized, followed by the formation of Mg₂AlOH and Mg₃OH environments in the LDH structure. This structure restoration from LDO to LDH should be associated with a retro-topotactic process, leading to a much shorter recovery time of ~6 h. Therefore, we believe that the solid-state recovery represents a true “memory effect” in which both long-range order and short-range order are recovered for LDH, while the conventional recovery process may not regenerate the original local structure (e.g., the distribution and ordering of cations due to the much less controlled dissolution and recrystallization in aqueous solution).

Compared to the conventional recovery, the solid-state recovery is much faster and only requires a very small amount of water, thus produces much less waste, it may provide a more environmentally friendly and economically feasible way for preparing LDH materials from LDOs^{41,42}. Therefore, the preparation of a variety of LDHs with different cations in the hydroxide sheets or interlayer anions have been attempted with this approach (Fig. 9 and Supplementary Fig. 14). The XRD patterns show that the conversion from LDOs to LDHs can be completed successfully in solid state. Therefore, this approach provides a green and robust method for the regeneration of LDH materials.

Discussion

In conclusion, the structure evolution of the memory effect from Mg/Al-LDO to Mg/Al-LDH can be successfully probed by applying ex situ and in situ solid-state NMR spectroscopy. Differences in the structure regeneration time and the formation order of different hydroxyl species (Mg₃OH and Mg₂AlOH) are found to be associated with the amount of water present in the structure reformation process. The conventional structural regeneration route in aqueous solution is associated with a dissolution-recrystallization mechanism, while the solid-state recovery is a direct retro-topotactic process, leading to a true “memory effect” and a much faster structure recovery of the latter. These results help to reconsider the role of water and show that the amount of water may be very important in controlling the interactions between water and oxides, thus the dominating memory effect mechanism for LDH. The characterization approach demonstrated in this study can be readily extended to investigate the details of the interactions of water with other oxides, and many other processes in which the different amounts of water may result in different mechanisms. Extension of this solid-state recovery of LDH from LDO can also provide a green preparation route for a variety of LDHs.

Methods

Preparation of the Mg/Al-LDH and Mg/Al-LDO

The Mg/Al-LDH with a Mg/Al molar ratio of 4.0 was prepared by coprecipitation method. Briefly, solution A was obtained by dissolving 0.016 mol Mg(NO₃)₂·6H₂O and 0.004 mol Al(NO₃)₃·9H₂O in 40 mL deionized water. Solution B was prepared by dissolving 0.04 mol NaOH in 40 mL deionized water. The two solutions were then added

drop by drop to a 250 mL flask under vigorous stirring at room temperature. At the same time, 0.5 M NaOH or 0.5 M HNO₃ solution was added dropwise to the mixture to maintain a pH of 10, which was monitored with a pH electrode (Mettler Toledo S40K). The mixture was then transferred to a 100 mL Teflon hydrothermal autoclave and heated at 180 °C for 24 h. After that, the product was centrifuged and washed with deionized water until the solution was neutral, and finally dried at 60 °C to obtain Mg/Al-LDH. Mg/Al-LDH was further calcined at 450 °C for 4 h and the product is denoted as Mg/Al-LDO.

Deuteration of Mg/Al-LDH

The as-synthesized Mg/Al-LDH was suspended in D₂O for deuteration. The mixture was stirred magnetically at 300 K for 48 h, before it was centrifuged and finally vacuum-dried at 333 K.

Basic characterization

The powder XRD data were obtained on a Shimadzu XRD-6000 diffractometer using Cu K α radiation ($\lambda = 1.5418$ Å) operating at 40 kV and 40 mA, with a scan step of 5° in the 2 θ range from 2° (or 5°) to 70°. Transmission electron microscopy (TEM) images were obtained using a JEM-2010 electron microscope (JEOL, Tokyo, Japan) at 200 kV, where the samples were dispersed by ultrasonic oscillation. The Mg and Al molar percentages were determined by inductively coupled plasma (ICP) emission spectroscopy (Perkin-Elmer ICP OPTIMA-5300DV). The N (nitrate) contents were determined by elemental analysis (Elementar Vario MICRO). The thermogravimetric profile of each sample was collected on a thermal analysis system (NETZSCH STA 449 C) in a N₂ atmosphere at a ramping rate of 10 °C/min from 30 to 700 °C.

Solid-state NMR experiments

Solid-state NMR experiments at 9.4 T were performed using a Bruker Avance III spectrometer and a 3.2 mm double resonance probe. ¹H MAS NMR spectra was collected with a rotor-synchronized spin echo sequence ($\pi/2 - \tau - \pi - \tau - \text{acq}$, $\tau =$ one rotor period) at a MAS rate of 20 kHz with a recycle delay of 2 s. ²⁷Al MAS NMR spectra were obtained with a single pulse sequence with ¹H decoupling during acquisition at a MAS rate of 20 kHz with a recycle delay of 0.2 s. ¹H and ²⁷Al shifts were referenced to external standards of H₂O and 0.1 M Al(NO₃)₃ aqueous solution at 4.8 and 0.0 ppm, respectively. The ¹H/²⁷Al TRAPDOR (TRAnSfer of Population in DOuble Resonance) experiments were carried out at a spinning speed of 5 kHz and a recoupling time of 0.2 and 2 ms with an rf field of 60 kHz for ²⁷Al irradiation. All NMR spectra were corrected for this background resonance by subtracting the empty rotor spectrum.

Ex situ XRD/NMR experiments

Ex situ XRD/NMR experiments were performed on Mg/Al-LDO samples with different rehydration time t at about 300 K (room temperature). Briefly, 100 mg Mg/Al-LDO was added to 10 mL NaNO₃ solution in D₂O (mass ratio of Mg/Al-LDO to D₂O: -1/100), and after a specific time t the solid was recovered by centrifugation before it was washed with deionized water or D₂O.

In situ solid-state NMR experiments

For in situ solid-state NMR experiments, 12 mg Mg/Al-LDO was packed in a zirconia rotor before 12 μ L NaNO₃ solution in D₂O was added to the rotor (solid/liquid: -1/1), which is followed by in situ NMR investigations. The rotor was spun at 20 kHz for in situ NMR data acquisition (temperature is measured as ~303 K at a MAS rate of 20 kHz). Considering the time (~2 min) for putting the rotor in the probe and tuning the instrument ready for data collection, the first ¹H NMR spectrum was obtained with a rehydration time t of 2–4 min. After that, ¹H NMR spectra were acquired every 2, 10, and 60 min in the first 10 min, 10–60 min, and after 60 min, respectively.

Data availability

All data supporting the findings presented here are included in the manuscript, its supporting information, or from the authors upon request.

References

1. Fan, G., Li, F., Evans, D. G. & Duan, X. Catalytic applications of layered double hydroxides: recent advances and perspectives. *Chem. Soc. Rev.* **43**, 7040–7066 (2014).
2. Chen, H., Hu, L., Chen, M., Yan, Y. & Wu, L. Nickel-cobalt layered double hydroxide nanosheets for high-performance supercapacitor electrode materials. *Adv. Funct. Mater.* **24**, 934–942 (2014).
3. Chen, G. et al. Accelerated hydrogen evolution kinetics on nife-layered double hydroxide electrocatalysts by tailoring water dissociation active sites. *Adv. Mater.* **30**, 1706279 (2018).
4. Wang, Q. & O'Hare, D. Recent advances in the synthesis and application of layered double hydroxide (LDH) nanosheets. *Chem. Rev.* **112**, 4124–4155 (2012).
5. Gong, M. et al. An advanced Ni-Fe layered double hydroxide electrocatalyst for water oxidation. *J. Am. Chem. Soc.* **135**, 8452–8455 (2013).
6. Coq, B., Tichit, D. & Ribet, S. Co/Ni/Mg/Al layered double hydroxides as precursors of catalysts for the hydrogenation of nitriles: hydrogenation of acetonitrile. *J. Catal.* **189**, 117–128 (2000).
7. Ma, H., Wang, H., Wu, T. & Na, C. Highly active layered double hydroxide-derived cobalt nano-catalysts for p-nitrophenol reduction. *Appl. Catal. B-Environ.* **180**, 471–479 (2016).
8. Liu, Y., Yang, Z., Xie, X., Huang, J. & Wen, X. Layered double oxides nano-flakes derived from layered double hydroxides: preparation, properties and application in zinc/nickel secondary batteries. *Electrochim. Acta* **185**, 190–197 (2015).
9. Guo, Y., Zhu, Z., Qiu, Y. & Zhao, J. Enhanced adsorption of acid brown 14 dye on calcined Mg/Fe layered double hydroxide with memory effect. *Chem. Eng. J.* **219**, 69–77 (2013).
10. Zhu, M. X., Li, Y. P., Xie, M. & Xin, H. Z. Sorption of an anionic dye by uncalcined and calcined layered double hydroxides: a case study. *J. Hazard. Mater.* **120**, 163–171 (2005).
11. Jin, L., Huang, Q.-J., Zeng, H.-Y., Du, J.-Z. & Xu, S. Organic modification of Mo-decorated MgAl layered double hydroxide for polymer flame retardancy. *Compos. Part A-Appl. S* **129**, 105717 (2020).
12. Rao, K. K., Gravelle, M., Valente, J. S. & Figueras, F.C. Activation of Mg–Al hydrotalcite catalysts for aldol condensation reactions. *J. Catal.* **173**, 115–121 (1997).
13. Zhao, L. et al. Investigating local structure in layered double hydroxides with ^{17}O NMR Spectroscopy. *Adv. Funct. Mater.* **24**, <https://doi.org/10.1002/adfm.201301157> (2014).
14. Kowalik, P. et al. Memory effect of the CuZnAl-LDH derived catalyst precursor—In situ XRD studies. *Appl. Catal. A-Gen.* **464–465**, 339–347 (2013).
15. Bokhoven, J. A. V., Roelofs, J. C. A. A., Jong, K. P. D. & Koningsberger, D. C. Unique structural properties of the mg±al hydrotalcite solid base catalyst: an in situ study using mg and al k-edge xafs during calcination and rehydration. *Chem. Eur. J.* **7**, 1258–1265 (2001).
16. Valente, J. S. et al. Comprehending the thermal decomposition and reconstruction process of sol-gel MgAl layered double hydroxides. *J. Phys. Chem. C* **114**, 2089–2099 (2010).
17. Gao, Z., Sasaki, K. & Qiu, X. Structural memory effect of Mg-Al and Zn-Al layered double hydroxides in the presence of different natural humic acids: process and mechanism. *Langmuir* **34**, 5386–5395 (2018).
18. Sato, T., Fujita, H., Endo, T., Shimada, M. & Tsunashima, A. Synthesis of hydrotalcite-like compounds and their physico-chemical properties. *Reactivity Solids* **5**, 219–228 (1988).
19. Takehira, K. et al. Mechanism of reconstitution of hydrotalcite leading to eggshell-type Ni loading on MgAl mixed oxide. *J. Catal.* **231**, 92–104 (2005).
20. Ye, H. et al. Regeneration mechanism, modification strategy, and environment application of layered double hydroxides: Insights based on memory effect. *Coord. Chem. Rev.* **450**, 214253 (2022).
21. Radha, A. V., Kamath, P. V. & Shivakumara, C. Order and disorder among the layered double hydroxides: combined Rietveld and DIFFaX approach. *Acta Crystallogr. B* **63**, 243–250 (2007).
22. Pushparaj, S. S. C. et al. How the method of synthesis governs the local and global structure of zinc aluminum layered double hydroxides. *J. Phys. Chem. C* **119**, 27695–27707 (2015).
23. Zhao, E. W. et al. In situ NMR metrology reveals reaction mechanisms in redox flow batteries. *Nature* **579**, 224–228 (2020).
24. Key, B. et al. Real-time NMR investigations of structural changes in silicon electrodes for lithium-ion batteries. *J. Am. Chem. Soc.* **131**, 9239–9249 (2009).
25. Sideris, P. J., Nielsen, U. G., Gan, Z. & Grey, C. P. Mg/Al ordering in layered double hydroxides revealed by multinuclear NMR spectroscopy. *Science* **321**, 113–117 (2008).
26. Staal, L. B. et al. Competitive reactions during synthesis of zinc aluminum layered double hydroxides by thermal hydrolysis of urea. *J. Mater. Chem. A* **5**, 21795–21806 (2017).
27. Sideris, P. J., Blanc, F., Gan, Z. & Grey, C. P. Identification of cation clustering in Mg–Al layered double hydroxides using multinuclear solid state nuclear magnetic resonance spectroscopy. *Chem. Mater.* **24**, 2449–2461 (2012).
28. Yu, G. et al. Probing local structure of layered double hydroxides with $(1)\text{h}$ solid-state nmr spectroscopy on deuterated samples. *J. Phys. Chem. Lett.* **5**, 363–369 (2014).
29. Yu, G. et al. Dehydration and dehydroxylation of layered double hydroxides: new insights from solid-state nmr and ft-ir studies of deuterated samples. *J. Phys. Chem. C* **119**, 12325–12334 (2015).
30. Cadars, S. et al. Identification and quantification of defects in the cation ordering in mg/al layered double hydroxides. *Chem. Mater.* **23**, 2821–2831 (2011).
31. Meyn, M., Beneke, K. & Lagaly, G. Anion-exchange reactions of layered double hydroxides. *Inorg. Chem.* **29**, 5201–5207 (1990).
32. Jana, A. et al. In-situ polymerization into the basal spacing of LDH for selective and enhanced uranium adsorption: a case study with real life uranium alkaline leach liquor. *Chem. Eng. J.* **428**, 131180 (2022).
33. Jiang, G. et al. MgAl layered double oxide: one powerful sweeper of emulsified water and acid for oil purification. *J. Hazard. Mater.* **367**, 658–667 (2019).
34. Chizallet, C. et al. Study of the structure of OH Groups on MgO by 1D and 2D ^1H MAS NMR combined with DFT cluster calculations. *J. Phys. Chem. C* **111**, 18279–18287 (2007).
35. Vyalikh, A. et al. From layered double hydroxides to layered double hydroxide-based nanocomposites a solid-state NMR study. *J. Phys. Chem. C* **113**, 21308–21313 (2009).
36. Grey, C. P. & Vega, A. J. Determination of the quadrupole coupling constant of the invisible aluminum spins in zeolite HY with ^7WAl TRAPDOR NMR. *J. Am. Chem. Soc.* **117**, 8232–8242 (1995).
37. Díez, V. K., Apesteguía, C. R. & Cosimo, J. I. D. Effect of the chemical composition on the catalytic performance of MgyAlO_x catalysts for alcohol elimination reactions. *J. Catal.* **215**, 220–233 (2003).
38. Yesinowski, J. P., Eckert, H. & Rossmant, G. R. Characterization of hydrous species in minerals by high-speed ^1H MAS-NMR. *J. Am. Chem. Soc.* **110**, 1367–1375 (1988).
39. Fraissard, J. & Batamack, P. ^1H -NMR study of heterogeneous adsorbent-adsorbate (water, methanol) equilibria at 4 K:

- application to the acid strength of solids. *Colloid Surf. A* **158**, 211–220 (1999).
40. Chen, J. et al. Interactions of oxide surfaces with water revealed with solid-state NMR spectroscopy. *J. Am. Chem. Soc.* **142**, 11173–11182 (2020).
41. Hu, Z. et al. Rapid mass production of two-dimensional metal oxides and hydroxides via the molten salts method. *Nat. Commun.* **8**, 15630 (2017).
42. Zhang, X., Qi, F., Li, S., Wei, S. & Zhou, J. A mechanochemical approach to get stunningly uniform particles of magnesium–aluminum-layered double hydroxides. *Appl. Surf. Sci.* **259**, 245–251 (2012).

Acknowledgements

This work was supported by the National Key R&D Program of China (2021YFA1502803), the National Natural Science Foundation of China (NSFC) (21972066, 22272075 and 91745202), NSFC-Royal Society Joint Program (21661130149). Luming Peng thanks the Royal Society and Newton Fund for a Royal Society - Newton Advanced Fellowship. This work was also supported by the Research Funds for the Frontiers Science Center for Critical Earth Material Cycling, Nanjing University and a Project Funded by the Priority Academic Program Development of Jiangsu Higher Education Institutions.

Author contributions

L.J., X.Z., and F.W. conducted the LDHs preparation and characterization, L.J., X.N., Y.W., B.S., C.Y., X.K., and D.W. carried out the solid-state NMR experiments; L.J. and L.P. designed the project and wrote the manuscript.

Competing interests

The authors declare no competing interests.

Additional information

Supplementary information The online version contains supplementary material available at <https://doi.org/10.1038/s41467-022-33912-7>.

Correspondence and requests for materials should be addressed to Luming Peng.

Peer review information *Nature Communications* thanks Yining Huang and the other, anonymous, reviewer(s) for their contribution to the peer review of this work.

Reprints and permission information is available at <http://www.nature.com/reprints>

Publisher's note Springer Nature remains neutral with regard to jurisdictional claims in published maps and institutional affiliations.

Open Access This article is licensed under a Creative Commons Attribution 4.0 International License, which permits use, sharing, adaptation, distribution and reproduction in any medium or format, as long as you give appropriate credit to the original author(s) and the source, provide a link to the Creative Commons license, and indicate if changes were made. The images or other third party material in this article are included in the article's Creative Commons license, unless indicated otherwise in a credit line to the material. If material is not included in the article's Creative Commons license and your intended use is not permitted by statutory regulation or exceeds the permitted use, you will need to obtain permission directly from the copyright holder. To view a copy of this license, visit <http://creativecommons.org/licenses/by/4.0/>.

© The Author(s) 2022